Available online at www.sciencedirect.com
ScienceDirect
International Journal of Heat and Mass Transfer 50 (2007) 1106–1121
International Journal of HEAT and MASS TRANSFER
www.elsevier.com/locate/ijhmt

Heat transfer with laminar forced convection in a porous channel exposed to a thermal asymmetry

J. Mitrovic *, B. Maletic

Institut für Energie-und Verfahrenstechnik, Thermische Verfahrenstechnik und Anlagentechnik, Universität Paderborn, 33095 Paderborn, Germany

Received 15 December 2005; received in revised form 6 June 2006
Available online 23 October 2006

Abstract

The effect of thermal asymmetry on laminar forced convection heat transfer in a plane porous channel with Darcy dissipation has been investigated numerically. The parallel plates making the channel boundaries were kept at constant, but different temperatures. The thermal asymmetry thus imposed on the system, results in an asymmetric temperature field and different heat fluxes across the channel boundaries. Depending on Darcy, Peclét and Reynolds number, the thermal asymmetry may lead to a reversal of the heat flux at a certain position along the flow at least at one of the channel walls. The corresponding Nusselt numbers become zero and might experience discontinuities thereby jumping from infinite positive to infinite negative, or vice versa. This feature is observed not only in the region of thermal development, but also in the fully developed region. In the fully developed region, an analytical expressions for the Nusselt numbers were obtained. From these expressions, analytical equations were deduced for the calculations of the axial positions along the channel where the Nusselt numbers become zero, or experiences discontinuity.

Keywords: Porous media; Laminar developing flow; Heat transfer; Thermal asymmetry

1. Introduction

The heat transfer with forced convection in porous media is an interesting and challenging physical problem, the solution of which is important in several areas of engineering practice, see e.g. Bejan et al. [1]. It has, therefore, extensively been studied in the past, and various fluid flow and heat transfer arrangements have been treated both analytically and numerically, see e.g. Kaviany [2], Nield and Bejan [3], Bejan [4] and Vafai [5]. However, the problem is far from being completely solved, even the governing equations are still the subject matter of scientific debates, see e.g. Travkin and Catton [6], Gray and Miller [7], Bear and Bachmat [8], and Whitaker [9]. Nevertheless, the mathematical models used so far account for different effects and the solutions obtained are adapted to various boundary conditions. For instance, Kaviany [10] studied laminar forced convection in a porous channel bounded by isothermal parallel plates adopting the Brinkman-extended Darcy model. Vafai and Kim [11] arrived at a closed form solution with fully developed forced convection in a porous plane channel exposed to a symmetric heating at constant heat flux. Nield et al. [12] analysed the fully developed forced convection in a fluid-saturated porous-medium channel with isothermal or isoflux boundaries. Nield et al. [13] investigated the heat transfer in a thermally developing region of a hydrodynamically developed flow in a plane porous channel bounded by isothermal plates. The energy equation they used accounts for viscous dissipation and axial heat conduction. The solutions reported illustrate the effects of Brinkman, Peclét and Darcy numbers on the heat transfer for different dissipation models. Mohamad [14] investigated the flow field and heat transfer with laminar forced convection in conduits filled with a porous material to different degrees. As far as the homogeneously filled channel is concerned, the effect of Darcy number on heat transfer in the fully developed flow region may largely

* Corresponding author. Tel.: +49 5251 60 2409; fax: +49 5251 60 3207.
E-mail address: mitrovic@tvt.upb.de (J. Mitrovic).

0017-9310/$ - see front matter © 2006 Elsevier Ltd. All rights reserved.
doi:10.1016/j.ijheatmasstransfer.2006.06.046

Nomenclature

c_p	specific heat at constant P
CP	cold plate
C_1	constant
C_2	constant
Da	Darcy number, Eq. (6)
Ec	Eckert number, Eq. (6)
HP	hot plate
k	thermal conductivity
K	permeability of porous medium
m	inverse square root of Da, Eq. (9)
M	viscosity ratio, Eq. (9)
Nu	Nusselt number, Eqs. (23) and (24)
p	dimensionless pressure, Eq. (6)
P	pressure
Pe	Peclét number, Eq. (6)
Pr	Prandtl number
q	heat flux
Re	Reynolds number, Eq. (6)
T	temperature
u	dimensionless velocity
U	velocity
W	half width of channel
x	dimensionless axial coordinate
X	axial coordinate
y	dimensionless cross coordinate
Y	cross coordinate
ε	heat source strength, Eq. (3)
σ	pressure drop function, Eq. (6)
κ	thermal diffusivity
ν	kinematic viscosity
μ	dynamic viscosity
θ	dimensionless temperature with thermal asymmetry, Eq. (6)
Θ	dimensionless temperature with thermal symmetry, Eq. (64)
ρ	density
Ω	parameter, Eqs. (17) and (64)
ξ	dimensionless axial coordinate, Eq. (18)
ψ	scaled temperature difference with thermal asymmetry, Eq. (18)
Ψ	scaled temperature difference with thermal symmetry, Eq. (64)

Indices

eff	effective property
C	cold
H	hot
IN	inlet
m	average
SL	slip flow
W	wall

be neglected for $Da > 1$. Haji-Sheikh and Vafai [15] performed heat transfer analysis on various cross sections of the conduits without a heat source giving detailed insights into the effect of Darcy number on thermal performance of porous inserts. For this model, Haji-Shekh [16] provided approximate expression for the Nusselt number.

When treating transport processes in porous media the so-called *Local Thermal Equilibrium* model (LTE) is frequently adopted. By this model, the fluid and the porous medium are considered as a single phase having physical properties of the actual phases mostly weighted by the volume fractions occupied by these phases. The applicability of this model is confined to a certain range of process and system parameters like fluid velocity and transport properties of the phases. Contrary to this model, the model of *Local Thermal Non-Equilibrium* (LTNE) accounts for thermal interaction among the phases within the porous system [17–23]. By this model the thermal interaction is based on a heat transfer coefficient at the phase interface within the porous system which is previously unknown. The LTNE two equations model is usually considered to be more adequate than the one equation LTE model. The boundary between these models regarding their applicability has been discussed in several papers, see e.g. Kim and Jang [19] and the references therein.

In summary, the treatments in all of the above mentioned references are restricted to thermally symmetric boundary conditions. In practice, however, it is indeed almost impossible to accomplish such conditions, and thermal asymmetry will probably be the rule rather than exception. Thermal asymmetry is shown by Mitrovic and Maletic [24] to materially affect the heat transfer in laminar forced convection in a conduit of annular cross section without a porous insert, and similar effects of thermal asymmetry may also be expected in the case of porous channels. Mahmud and Fraser [25] studied the heat transfer and entropy generation with laminar fully developed flow in a porous channel bounded by parallel plates, which were kept isothermal at different temperatures thus imposing on the system a thermal asymmetry. The inertia in the momentum equation was disregarded, while a volumetric source term was included into the energy equation. The physical properties were taken as constant, so the flow field is decoupled from the temperature field, and the one-dimensional transport equations were solved analytically. The thermal asymmetry results in an asymmetric temperature distribution in the porous gap the shape of which depends on the Eckert, the Prandtl and the Darcy number. Consequently, it also affects the heat transfer across the porous insert. The analysis of Mahmud and Fraser [25] is

restricted to the cold plate. Xiong and Kuznetsov [26] investigated thermal dispersion and non Darcian effects with forced convection in a Couette flow in a composite flat conduit. The walls were kept at constant but different heat fluxes. Mitrovic and Maletic [27] performed a detailed heat transfer analysis with laminar forced convection in a porous annular channel with Darcy dissipation.

Detailed considerations of forced convection heat transfer in a porous flat channel exposed to a thermal asymmetry at constant wall temperatures do not seem to exist in the literature. This paper provides an analysis of the issue, assuming a hydrodynamically developed steady-state laminar flow. The porous insert of homogeneous permeability is sandwiched between two parallel plates that are at constant, but different temperatures. The heat source corresponds to the Darcy model, the axial heat conduction being neglected. The problem is treated on the basis of the LTE model numerically by using Mathematica [28]. A closed solution of the energy equation was obtained in the fully developed region. As is demonstrated in this paper, the thermal asymmetry substantially affects the heat transfer. Depending on Darcy, Eckert and Peclét number, the thermal asymmetry can lead to a reversal of the heat flux with discontinuities of the Nusselt numbers on both plates.

2. Physical model and governing equations

The physical model is illustrated in Fig. 1. Two parallel plates of constant temperatures T_C and $T_H \neq T_C$ sandwich a porous layer of a thickness 2 W saturated with a Newtonian fluid flowing along the X-coordinate. The plates are infinite in the direction orthogonal to the $X0Y$-plane, the flow and temperature fields depend only on X and Y. After a sufficiently large flow length downstream the channel inlet, in the fully developed region, these fields become independent of X.

The following assumptions are adopted:

- the permeability of the porous medium is homogeneous,
- the physical properties are constant,
- free convection effects are neglected,
- the fluid temperature and velocity are constant in the inlet cross-section,
- the phases are locally at thermal equilibrium,
- the heat source term corresponds to the Darcy flow model,
- the system is at steady-state,
- the fluid flow is taken as one-dimensional and developed,
- the axial heat conduction is neglected.

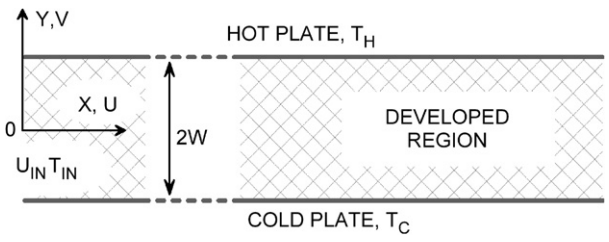

Fig. 1. Physical system.

With these assumptions, the fluid flow is described by the Brinkman momentum equation, see e.g. Nield et al. [13],

$$\mu_{\text{eff}}\frac{\partial^2 U}{\partial Y^2}-\frac{\mu}{K}U-\frac{\partial P}{\partial X}=0, \tag{1}$$

whereas the heat transfer obeys the following energy equation,

$$U\frac{\partial T}{\partial X}=\kappa\frac{\partial^2 T}{\partial Y^2}+\frac{\varepsilon}{\rho c_p}. \tag{2}$$

Here μ_{eff} denotes an effective viscosity, U the axial velocity, μ the dynamic fluid viscosity, K the permeability of the porous medium, P the pressure, T the temperature and ε a volumetric heat source; κ, ρ and c_p are the usual fluid properties, X and Y follow from Fig. 1.

The simplest expression for ε is [13]

$$\varepsilon=\frac{\mu}{K}U^2. \tag{3}$$

Eqs. (1) and (2) can be written non-dimensional as follows

$$\frac{\partial^2 u}{\partial y^2}-\frac{\mu}{\mu_{\text{eff}}}\frac{u}{Da}-Re\frac{\mu}{\mu_{\text{eff}}}\frac{\partial p}{\partial x}=0, \tag{4}$$

$$Peu\frac{\partial\theta}{\partial x}=\frac{\partial^2\theta}{\partial y^2}+\frac{Ec\,Pr}{Da}u^2, \tag{5}$$

where the non-dimensional quantities are defined by

$$\begin{aligned} &x=\frac{X}{W},\quad y=\frac{Y}{W},\quad u=\frac{U}{U_{IN}},\quad Re=\frac{U_{IN}W}{\nu},\\ &Da=\frac{K}{W^2},\quad p=\frac{P}{\rho U_{IN}^2},\quad Pe=\frac{U_{IN}W}{\kappa},\quad \theta=\frac{T-T_{IN}}{T_H-T_{IN}}\\ &Ec=\frac{U_{IN}^2}{c_p(T_H-T_{IN})},\quad Pr=\frac{\nu}{\kappa}. \end{aligned} \tag{6}$$

The indices H and IN refer to the hot plate and the channel inlet, respectively. Note that the definitions of the Eckert number Ec and the temperature θ are inappropriate at $T_H = T_{IN}$.

3. Flow field and pressure drop

With the boundary conditions

$$\begin{aligned} &Y=+W,\quad y=+1:\quad U=0,\quad u=0,\\ &Y=-W,\quad y=-1:\quad U=0,\quad u=0, \end{aligned} \tag{7}$$

the solution of Eq. (1) is

$$u=\frac{\Phi}{m^2}\left(1-\frac{\cosh(my)}{\cosh m}\right)=\frac{\Phi}{m^2}\left(1-\frac{e^{my}+e^{-my}}{2\cosh m}\right), \tag{8}$$

$$-Re\frac{\mu}{\mu_{\text{eff}}}\frac{\partial p}{\partial x}=\Phi,\quad m^2=\frac{1}{Da}\frac{\mu}{\mu_{\text{eff}}}=\frac{1}{Da\,M}. \tag{9}$$

Averaging the velocity u over the channel width results in an expression for the pressure drop function Φ,

$$U_m = \frac{1}{2W}\int_{-W}^{+W} U\,\mathrm{d}Y = \frac{1}{2}U_{IN}\int_{-1}^{+1} u\,\mathrm{d}y, \tag{10}$$

$$\frac{1}{2}\int_{-1}^{+1} u\,\mathrm{d}y = \frac{U_m}{U_{IN}} = 1, \tag{11}$$

$$\frac{\Phi}{m^2}\left(1 - \frac{\sinh m}{m\cdot\cosh m}\right) = 1, \tag{12}$$

$$\Phi = \frac{m^2}{1 - \frac{\sinh m}{m\cdot\cosh m}} = \frac{1/(Da\,M)}{1 - \sqrt{Da\,M}\,\frac{\sinh(1/\sqrt{Da\,M})}{\cosh(1/\sqrt{Da\,M})}}. \tag{13}$$

Fig. 2 illustrates Eq. (13). Mahmud and Fraser [25] proposed correlations for the pressure drop function $\Phi(M=1)$ which are valid piece-wise along the parameter Da. Their limit value of Φ at $Da\to\infty$ reported to be $\Phi = 2.95$ is slightly lower than the exact limit value of $\Phi = 3.0$ deduced from Eq. (13), thus

$$\Phi = -Re\frac{\mu}{\mu_{\mathrm{eff}}}\frac{\partial p}{\partial x} = -\frac{Re}{M}\frac{\partial p}{\partial x} = 3, \quad DaM\to\infty. \tag{14}$$

4. General expressions for temperature field and heat transfer

Inserting the expression (8) for the velocity u in Eq. (2) gives

$$\frac{Pe\Phi}{m^2}f(m,y)\frac{\partial\theta}{\partial x} = \frac{\partial^2\theta}{\partial y^2} + \frac{EcPr\Phi^2}{m^2}\frac{\mu_{\mathrm{eff}}}{\mu}f^2(m,y), \tag{15}$$

$$f(m,y) = 1 - \frac{\cosh(my)}{\cosh m}. \tag{16}$$

Introducing

$$\Omega = \frac{EcPr\Phi^2}{m^2}\frac{\mu_{\mathrm{eff}}}{\mu}, \tag{17}$$

$$\psi = \frac{\theta}{\Omega}, \quad \xi = \frac{x}{Pe}, \tag{18}$$

Eq. (15) takes the form

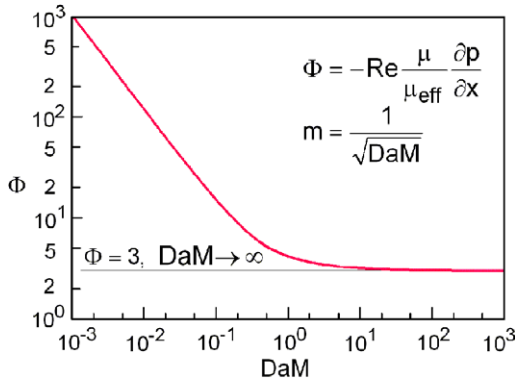

Fig. 2. Pressure drop characteristic Φ as function of Darcy number Da.

$$f(m,y)\frac{\Phi}{m^2}\frac{\partial\psi}{\partial\xi} = \frac{\partial^2\psi}{\partial y^2} + f^2(m,y). \tag{19}$$

The boundary conditions to be satisfied are

$$\begin{aligned} &y=+1:\ \theta = (T_H - T_{IN})/(T_H - T_{IN}) = 1, \quad \psi = 1/\Omega = \psi_H,\\ &y=-1:\ \theta = (T_C - T_{IN})/(T_H - T_{IN}) = \theta_C, \quad \psi = \theta_C/\Omega = \psi_C. \end{aligned} \tag{20}$$

The quantity ψ represents the non-dimensional temperature difference scaled by the parameter Ω. The field of this quantity obtained from Eq. (19) coincides with the temperature field for $\Omega = 1$. For other values of the parameter Ω, the temperature field is correspondingly stretched, or compressed. The mean fluid temperature is obtained from

$$\theta_m = \frac{1}{2}\int_{-1}^{+1} u\theta\,\mathrm{d}y, \quad \psi_m = \frac{1}{2}\int_{-1}^{+1} u\psi\,\mathrm{d}y \tag{21}$$

and the Fourier heat flux q is calculated by

$$q = -k\frac{\partial T}{\partial Y} = -k\frac{T_H - T_{IN}}{W}\frac{\partial\theta}{\partial y}, \tag{22a}$$

$$\frac{qW}{k(T_H - T_{IN})} = -\frac{\partial\theta}{\partial y} = -\Omega\frac{\partial\psi}{\partial y}, \tag{22b}$$

giving the Nusselt number Nu at the channel boundary

$$\begin{aligned} Nu_H &= \frac{W}{k}\frac{q}{T_H - T_m} = -\frac{1}{1-\theta_m}\left(\frac{\partial\theta}{\partial y}\right)_H\\ &= -\frac{1}{\psi_H - \psi_m}\left(\frac{\partial\psi}{\partial y}\right)_H, \end{aligned} \tag{23}$$

$$\begin{aligned} Nu_C &= \frac{W}{k}\frac{q}{T_C - T_m} = -\frac{1}{\theta_C - \theta_m}\left(\frac{\partial\theta}{\partial y}\right)_C\\ &= -\frac{1}{\psi_C - \psi_m}\left(\frac{\partial\psi}{\partial y}\right)_C, \end{aligned} \tag{24}$$

where the indices H and C refer to the hot ($y=+1$) and cold ($y=-1$) boundary, respectively.

5. Representative results

Eq. (19) can be solved by the method of separation of variables, as has been demonstrated by Lahjomri et al. [29,30] and Nield et al. [13] for the symmetric thermal boundary conditions. However, we prefer a numerical treatment by using Mathematica [28]. Prior to presenting the numerical results in the developing region, an analytical solution obtained in the thermally developed region will be illustrated for some sets of the process parameters.

5.1. Fully developed heat transfer region

The forced convection heat transfer in a porous channel described by Eq. (19) reduces in the fully developed region to a relatively simple problem of heat conduction in a plane wall with a heat source, the strength of which changes along the coordinate y. Heat transfer in this region has been treated by Mahmud and Fraser [25]. They used the

difference of the plate temperatures to define a heat transfer coefficient. This, however, is inappropriate when the temperature distribution in the porous layer passes a maximum and the heat generated inside the layer is dissipated across both plates. In the following, first a detailed solution of the energy equation is given.

5.1.1. Temperature distribution with thermal asymmetry

Setting $\partial\psi/\partial\xi = 0$ and considering the expression (16) for the function f, Eq. (19) becomes

$$\frac{\partial^2\psi}{\partial y^2} = -\left(1 - \frac{2}{\cosh m}\frac{e^{my}+e^{-my}}{2} + \frac{1}{4\cosh^2 m}(e^{2my}+e^{-2my}+2)\right). \tag{25}$$

Performing integration gives

$$\psi = -\left(\frac{y^2}{2} - \frac{2}{\cosh m}\frac{e^{my}+e^{-my}}{2m^2} + \frac{1}{4\cosh^2 m}\left(\frac{e^{2my}+e^{-2my}}{4m^2}+y^2\right)\right) + C_1 y + C_2 \tag{26a}$$

or

$$\psi = -\left(\frac{y^2}{2} - \frac{2}{m^2}\frac{\cosh(my)}{\cosh m} + \frac{1}{4\cosh^2 m}\left(\frac{2\cosh^2(my)-1}{2m^2}+y^2\right)\right) + C_1 y + C_2, \tag{26b}$$

$$\psi = -\left(\frac{y^2}{2} - \frac{2Da\,M\cosh(y/\sqrt{Da\,M})}{\cosh(1/\sqrt{Da\,M})} + \frac{(2\cosh^2(y/\sqrt{Da\,M})-1)Da\,M + 2y^2}{8\cosh^2(1/\sqrt{Da\,M})}\right) + C_1 y + C_2. \tag{26c}$$

The boundary conditions, Eq. (20), deliver the constants C_1 and C_2,

$$C_1 = \frac{1}{2}(\psi_H - \psi_C), \tag{27}$$

$$C_2 = \frac{1}{2}(\psi_H + \psi_C) + \left(\frac{1}{2} - \frac{7}{4m^2} + \frac{1}{4\cosh^2 m}\left(1 - \frac{1}{2m^2}\right)\right). \tag{28}$$

For the limit $m \to 0$, that is, for $Da\,M \to \infty$, Eq. (26) reduce to

$$\psi(m\to 0) = \frac{1}{2}(\psi_H + \psi_C) + \frac{1}{2}(\psi_H - \psi_C)y, \quad m \to 0\,(Da\,M \to \infty). \tag{29}$$

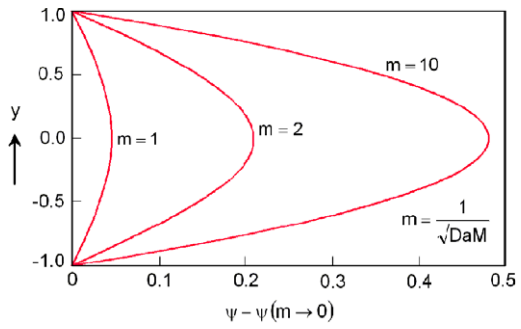

Fig. 3. Distribution of scaled temperature difference $\psi - \psi\ (m \to 0)$ in the porous layer.

Subtracting Eq. (29) from Eq. (26a) gives

$$\psi - \psi(m\to 0) = -\left(\frac{y^2}{2} - \frac{2}{\cosh m}\frac{e^{my}+e^{-my}}{2m^2} + \frac{1}{4\cosh^2 m}\left(\frac{e^{2my}+e^{-2my}}{4m^2}+y^2\right)\right) + F(m) \tag{30}$$

$$F(m) = \frac{1}{2} - \frac{7}{4m^2} + \frac{1}{4\cosh^2 m}\left(1 - \frac{1}{2m^2}\right). \tag{31}$$

As follows form Eq. (30), the scaled temperature difference $\psi - \psi\ (m \to 0)$ is symmetric with respect to the symmetry plane ($y = 0$) of the channel.

Fig. 3 shows the profiles of the scaled temperature difference $\psi - \psi\ (m \to 0)$ according to Eq. (30) for selected values of the parameter $m = 1/\sqrt{Da\,M}$, the variation of which results in different porosities and/or the channel widths. As follows from the diagram, the larger the parameter m is, the stronger the temperature change. For $m \to 0$, that is, for $Da\,M \to \infty$, the difference $\psi - \psi\ (m \to 0)$ becomes zero and the porous layer behaves like a solid wall or a channel flow without a heat source.

To throw some more light on the effect of thermal asymmetry on the temperature field, Eq. (30) is rearranged,

$$\theta = \frac{1}{2}(1+\theta_C) + \frac{1}{2}(1-\theta_C)y + \Omega\cdot(\psi - \psi(m\to 0)), \tag{32}$$

and regarding the specified temperatures (T_{IN},T_C,T_H), three cases are considered and illustrated in this paper:

$T_{IN} < T_C < T_H$: $0 < \theta_C < 1$, $\Omega > 0$

$T_C < T_{IN} < T_H$: $-\infty < \theta_C < 0$, $\Omega > 0$

$T_C < T_H < T_{IN}$: $1 < \theta_C < +\infty$, $\Omega < 0$.

For the purposes of the numerical evaluation, the parameters θ_C and Ω are chosen as follows:

$\theta_C = 0.5$, $\Omega = 5.0$

$\theta_C = -0.5$, $\Omega = 5.0$

$\theta_C = 2.0$, $\Omega = -5.0$.

Fig. 4 shows the temperature distributions for these parameter combinations. The straight line ($m = 0$) gives the temperature distribution in the channel without a porous insert [31]. As may be seen from the diagrams, the thermal asymmetry affects the temperature field significantly, and its deviation from the thermally symmetric field is larger at larger θ_C and/or m. The parameter m shapes the temperature distribution and determines the position of its maximum/minimum at given Ω. Note that Ω depends on m so, that a variation of m at fixed Ω actually corresponds to a variation of $Ec\,Pr\,M$,

$$Ec\,Pr\,M = \frac{\Omega}{m^2}\left(1 - \frac{\sinh m}{m\cdot\cosh m}\right)^2,$$

as follows from Eqs. (13) and (17).

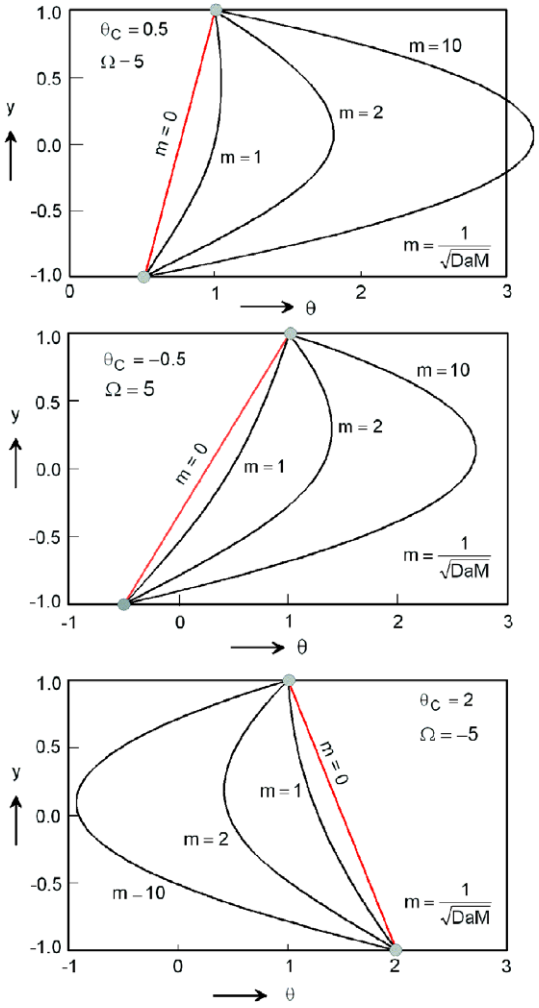

Fig. 4. Effect of thermal asymmetry and of the parameter m on the temperature distribution across the porous layer ($m = 0$: channel without porous insert).

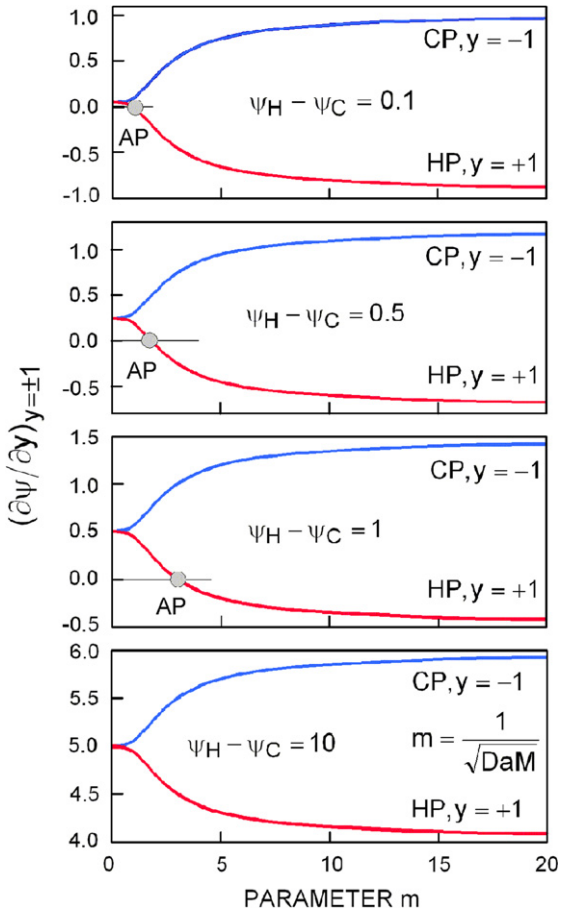

Fig. 5. Effect of thermal asymmetric on the dimensionless Fourier heat flux at the boundaries of the porous layer. The point AP on the curve indicates the adiabatic state.

5.1.2. Heat flux

By Eq. (22b), the heat flux q is proportional to the derivative $\partial\psi/\partial y$. For the latter, Eq. (26a) and the integration constants give

$$\frac{\partial\psi}{\partial y} = \frac{1}{2}(\psi_H - \psi_C) - \left(y - \frac{2}{\cosh m}\frac{e^{my} - e^{-my}}{2m} + \frac{1}{4\cosh^2 m}\left(\frac{e^{2my} - e^{-2my}}{2m} + 2y\right)\right) \tag{33a}$$

$$\frac{\partial\psi}{\partial y} = \frac{1}{2}(\psi_H - \psi_C) - \left(y - \frac{2}{m}\frac{\sinh(my)}{\cosh m} + \frac{1}{2\cosh^2 m}\left(\frac{\sinh(my)\cosh(my)}{m} + y\right)\right). \tag{33b}$$

At the hot plate, $y = +1$, it is

$$\left(\frac{\partial\psi}{\partial y}\right)_{y=+1} = \frac{1}{2}(\psi_H - \psi_C) - \left(1 - \frac{3}{2m}\frac{\sinh m}{\cosh m} + \frac{1}{2\cosh^2 m}\right), \tag{34}$$

and at the cold plate, $y = -1$,

$$\left(\frac{\partial\psi}{\partial y}\right)_{y=-1} = \frac{1}{2}(\psi_H - \psi_C) + \left(1 - \frac{3}{2m}\frac{\sinh m}{\cosh m} + \frac{1}{2\cosh^2 m}\right). \tag{35}$$

Fig. 5 illustrates the slopes $\partial\psi/\partial y = (\partial\theta/\partial y)/\Omega$ of the temperature profiles at the plates ($y = +1, y = -1$) as function of the parameter m, Eqs. (34) and (35), for the selected thermal asymmetries ($\psi_H - \psi_C$). The curves are symmetrical with respect to the line $\partial\psi/\partial y = (1/2)\cdot(\psi_H - \psi_C)$, which is the dimensionless heat flux in the channel without a porous insert,

$$\frac{qW}{k(T_H - T_{IN})} = -\frac{\partial\theta}{\partial y} = -\frac{1}{2}\Omega(\psi_H - \psi_C). \tag{36}$$

For sufficiently large m, the curves in Fig. 5 reach the asymptotes,

$$\left(\frac{\partial\psi}{\partial y}\right)_{y=\pm1} = \frac{1}{2}(\psi_H - \psi_C) \mp 1.$$

Above the symmetry line, the curves are valid for the cold plate (CP, $y = -1$), and the quantity $(\partial\psi/\partial y)_{y=+1}$ is positive for all values of the parameter Ω, which means that the porous layer always dissipates the heat across this plate. As is also obvious from this figure, in comparison to the

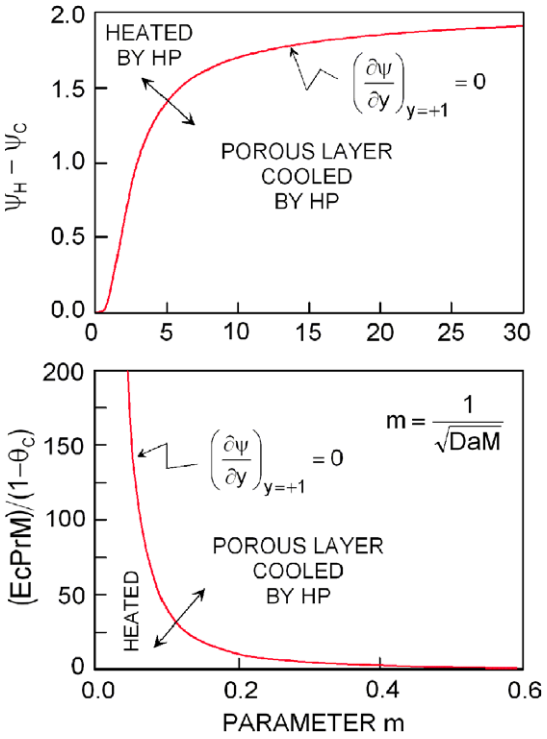

Fig. 6. Conditions for adiabatic hot plate ($y=+1$), implicit (above) and explicit (below) in parameter m.

case of an empty channel ($m=0$), the porous insert enhances the heat flux at the cold plate.

The situation is not as unique at the hot plate (HP, $y=+1$, curves below $\partial\psi/\partial y=(1/2)\cdot(\psi_H-\psi_C)$), Fig. 5. Since $(\psi_H-\psi_C)\geqslant 0$, $\partial\psi/\partial y$ may be positive, zero, or negative. This depends on the parameter m and the thermal asymmetry $(\psi_H-\psi_C)$. For $\partial\psi/\partial y>0$, the porous layer is heated by the hot plate, whereas for $\partial\psi/\partial y<0$, the porous layer dissipates the heat across this plate. For $\partial\psi/\partial y=0$, the hot plate is adiabatic, AP in the diagrams.

Fig. 6 illustrates the range of the parameters with heating or/and respectively cooling of the porous layer by the hot plate. The boundary between the two regions represents the adiabatic states of this plate, $(\partial\psi/\partial y)_{y=+1}=0$, or

$$\psi_H-\psi_C=2\cdot\left(1-\frac{3}{2m}\frac{\sinh m}{\cosh m}+\frac{1}{2\cosh^2 m}\right), \tag{37}$$

$$\frac{EcPrM}{1-\theta_C}=\frac{1}{2}\frac{m^2}{\Phi^2}\Big/\left(1-\frac{3}{2m}\frac{\sinh m}{\cosh m}+\frac{1}{2\cosh^2 m}\right). \tag{38}$$

For sufficiently large m, Eq. (37) reduces to

$$\psi_H-\psi_C=2\cdot\left(1-\frac{3}{2m}\right), \tag{39}$$

whereas Eq. (38) becomes

$$\frac{EcPrM}{1-\theta_C}=\frac{(m-1)^2}{(2m-1)m^3},\quad m\to\infty \tag{40}$$

$$\frac{EcPrM}{1-\theta_C}=\frac{1}{3m^2},\quad m\to 0. \tag{41}$$

The adiabatic state of the cold plate can easily be obtained from Eq. (35) resulting in an expression which is identical to Eq. (37), but with a negative right-hand side.

To gain further insights into the effect of thermal asymmetry on the heat flux, Eqs. (34) and (35) are multiplied by Ω giving the expressions

$$(\partial\theta/\partial y)_{y=+1}=\frac{1}{2}(1-\theta_C)-\frac{EcPrM\Phi^2}{m^2}\left(1-\frac{3}{2m}\frac{\sinh m}{\cosh m}+\frac{1}{2\cosh^2 m}\right), \tag{42}$$

$$(\partial\theta/\partial y)_{y=-1}=\frac{1}{2}(1-\theta_C)+\frac{EcPrM\Phi^2}{m^2}\left(1-\frac{3}{2m}\frac{\sinh m}{\cosh m}+\frac{1}{2\cosh^2 m}\right), \tag{43}$$

which are visualised in Fig. 7 for some values of $EcPrM\Phi^2$. A variation of this parameter shifts the curves up, or down. At $\theta_C>1$, the fluid inlet temperature is larger than the hot plate temperature and the lines representing the heat flux of this plate lie below the symmetry line.

For sufficiently large m, Eqs. (42) and (43) can be written as

$$\left(\frac{\partial\theta}{\partial y}\right)_{y=+1}=\frac{1}{2}(1-\theta_C)-\frac{2m-3}{2}\frac{m^3}{(m-1)^2}EcPrM, \tag{44}$$

$$\left(\frac{\partial\theta}{\partial y}\right)_{y=-1}=\frac{1}{2}(1-\theta_C)+\frac{2m-3}{2}\frac{m^3}{(m-1)^2}EcPrM, \tag{45}$$

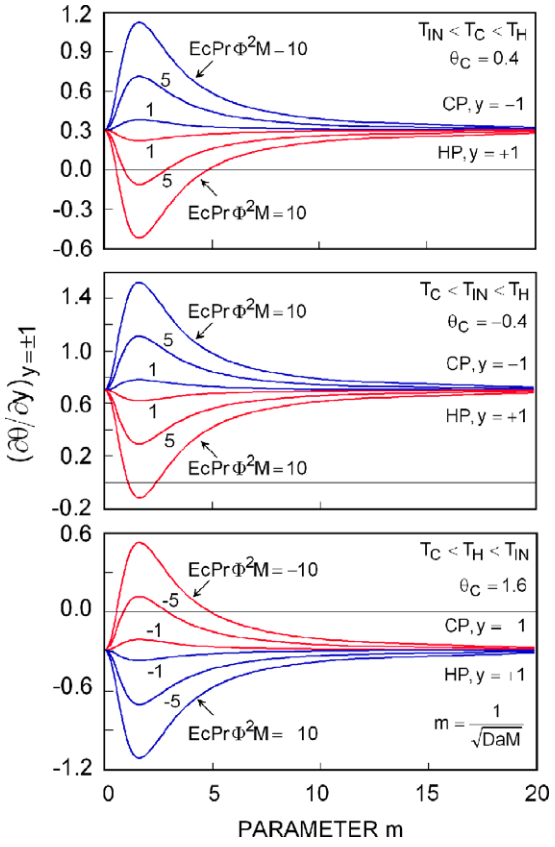

Fig. 7. Dimensionless heat fluxes at the boundaries for selected thermal asymmetries according to Eqs. (42) and (43).

and for $m \gg 3/2$, that is, for $Da\,M \ll 4/9$,

$$\left(\frac{\partial\theta}{\partial y}\right)_{y=+1} = \frac{1}{2}(1-\theta_C) - m^2 EcPrM = \frac{1}{2}(1-\theta_C) - \frac{EcPr}{Da}, \quad (46)$$

$$\left(\frac{\partial\theta}{\partial y}\right)_{y=-1} = \frac{1}{2}(1-\theta_C) + m^2 EcPrM = \frac{1}{2}(1-\theta_C) + \frac{EcPr}{Da}, \quad (47)$$

which for $Ec\,Pr/Da \to 0$ reduces to the case of an empty channel.

5.1.3. The Nusselt numbers

In the fully developed region, the average fluid temperature, defined in Eq. (21), can be obtained analytically,

$$\psi_M = \frac{\theta_m}{\Omega} = \frac{12(\psi_C+\psi_H)(m-\tanh m)m^2 + (4m^3-33)(2+\operatorname{sech}^2 m) + (88+\tanh^2 m + 17\operatorname{sech}^2 m)\tanh m}{24m^2(m-\tanh m)}. \quad (48)$$

With this expression for ψ_m, Eqs. (23) and (24) deliver

$$Nu_H = \frac{12(\psi_C-\psi_H)(m-\tanh m)m^2 + 12(2m+m\operatorname{sech}^2 m - 3\tanh m)(m-\tanh m)m}{2m(4m^2+6(\psi_C-\psi_H)m^2-33) + (89-12m^2(\psi_C-\psi_H))\tanh m + (4m^3-39m+16\tanh m)\operatorname{sech}^2 m}, \quad (49)$$

$$Nu_C = \frac{12(\psi_H-\psi_C)(m-\tanh m)m^2 - 12(2m+m\operatorname{sech}^2 m - 3\tanh m)(m-\tanh m)m}{2m(33+6(\psi_C-\psi_H)m^2-4m^2) - (88+12(\psi_C-\psi_H)m^2)\tanh m - \tanh^3 m + (39m-4m^3-17\tanh m)\operatorname{sech}^2 m}. \quad (50)$$

The Nusselt numbers Nu_H and Nu_C become zero when the plates become adiabatic, see Eq. (37) for the hot plate. In addition, setting in Eqs. (49) and (50) the denominators equal to zero, that is, equating the temperatures of the plates and the average fluid temperature ($\psi_H = \psi_m$, $\psi_C = \psi_m$), one obtains the vertical asymptotes of Nu_H and Nu_C:

$Nu_H = \pm\infty$:

$$\psi_H - \psi_C = \frac{8m^3 - 66m + (4m^3 - 39m + 16\tanh m)\operatorname{sech}^2 m + 89\tanh m}{12(m-\tanh m)m^2} \quad (51)$$

$Nu_C = \pm\infty$:

$$\psi_H - \psi_C = \frac{66m - 8m^3 - (4m^3 - 39m + 16\tanh m)\operatorname{sech}^2 m - 88\tanh m - \tanh^3 m}{12(m-\tanh m)m^2} \quad (52)$$

Fig. 8 illustrates the Nusselt numbers according to Eqs. (49) and (50) at the fluid inlet temperature below the plate temperatures, $T_{IN} < T_C < T_H$ for $\Omega = 1$ at selected values of ψ_C. Notice that for $\Omega = 1$, the quantity ψ is identical with the non-dimensional temperature θ. For the thermal symmetry ($\psi_C = \psi_H$, top diagram in Fig. 6), the Nusselt numbers Nu_H and Nu_C are equal, and they increase as the parameter m increases tending to the limit value $Nu_{H\infty} = Nu_{C\infty} = 3$, whereas for $m = 0$, $Nu_H = Nu_C = 1.886$, which is in agreement with the literature for an empty channel.

At a thermal asymmetry, the Nusselt number Nu_H experiences a discontinuity at a position that moves toward larger m as ψ_C decreases. At the thermal asymmetries ψ_C specified in Fig. 8, the Nusselt number Nu_H jumps from infinite negative to infinite positive. Further increase in the thermal asymmetry results in the appearance of an additional discontinuity of Nu_H, which then again disappears at stronger thermal asymmetry, Fig. 9.

The existence of the second discontinuity immediately follows from Fig. 10, where the thermal asymmetry $\psi_H - \psi_C$ given in Eq. (51) is plotted versus the parameter m at $Nu_H \to \infty$. As the Figure shows, two vertical asymptotes may establish at $\psi_H - \psi_C$ ranging from 2/3 to approximately 0.69.

5.1.4. Constant strength of heat source

A heat source of constant strength requires each quantity in the expression

$$\varepsilon = \frac{\mu}{K}U^2 = \text{const} \quad (53)$$

to be constant, or a variation of the ratio μ/K across the porous layer in a way that compensates the variation of the kinetic energy, $\mu/K \sim 1/U^2$.

Taking ε as function of y and averaging gives

$$\left(\frac{\mu}{K}\right)_m = \int_{-1}^{+1}\frac{\mu}{K}u^2\,\mathrm{d}y \Big/ \int_{-1}^{+1} u^2\,\mathrm{d}y, \quad (54)$$

which, for $u = 1$, that is for a slip flow, becomes

$$\left(\frac{\mu}{K}\right)_{SL} = \frac{1}{2}\int_{-1}^{+1}\frac{\mu}{K}\,\mathrm{d}y, \quad (55)$$

where the index SL refers to the slip flow.

With Eqs. (55) and (53) becomes

$$\varepsilon = \frac{\mu}{K}U_{IN}^2, \quad (56)$$

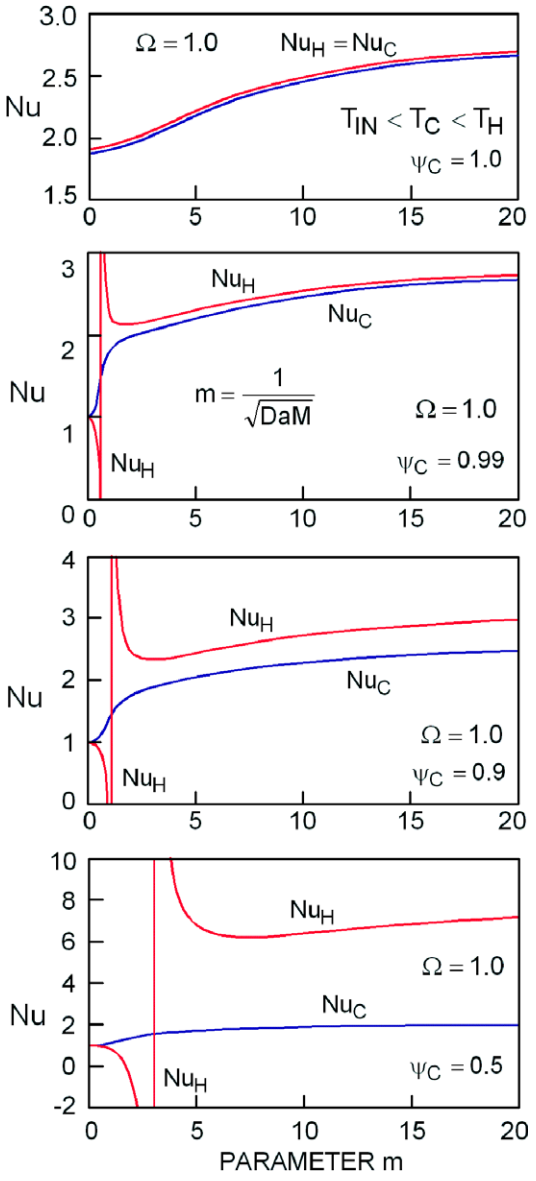

Fig. 8. Nusselt numbers Nu_H and Nu_C of the plates with fully developed flow at $T_{IN} < T_C < T_H$. For thermal symmetry, the curves coincide, but reason of illustration they are shifted slightly apart.

where the index SL is omitted, and, for $\partial\theta/\partial x = 0$, the energy Eq. (5) takes the form

$$\frac{\partial^2\theta}{\partial y^2} + \frac{Ec\,Pr}{Da} = 0. \tag{57}$$

The advantage of this equation is its simplicity, but its content is somewhat questionable, because, from the physical point of view, it is not easy to accept a piston-like flow of a viscous fluid in a porous matrix.

When integrated and adapted to the boundary condition (20), Eq. (57) gives

$$\theta = \frac{1}{2}\left(\frac{Ec\,Pr}{Da}(1-y^2) + (\theta_H - \theta_C)y + (\theta_H + \theta_C)\right). \tag{58}$$

The average temperature θ_m obtained from Eq. (21) at $u = 1$ is

$$\theta_m = \frac{1}{2}(\theta_H + \theta_C) + \frac{1}{3}\frac{Ec\,Pr}{Da}, \tag{59}$$

whereas the Nusselt numbers Nu_H and Nu_C, defined in Eqs. (23) and (24), become

$$Nu_H = -\frac{\frac{1}{2}(\theta_H - \theta_C) - \frac{Ec\,Pr}{Da}}{\frac{1}{2}(\theta_H - \theta_C) - \frac{1}{3}\frac{Ec\,Pr}{Da}}, \tag{60}$$

$$Nu_C = \frac{\frac{1}{2}(\theta_H - \theta_C) + \frac{Ec\,Pr}{Da}}{\frac{1}{2}(\theta_H - \theta_C) + \frac{1}{3}\frac{Ec\,Pr}{Da}}. \tag{61}$$

As $\theta_H > \theta_C$, the Nusselt number Nu_C of the cold plate is always positive and finite. On the contrary, the Nusselt number Nu_H of the hot plate becomes zero for

$$\frac{Ec\,Pr}{Da} = \frac{1}{2}(\theta_H - \theta_C), \tag{62}$$

and infinite at

$$\frac{Ec\,Pr}{Da} = \frac{3}{2}(\theta_H - \theta_C). \tag{63}$$

Fig. 11 illustrates Eqs. (60) and (61) showing the Nusselt number Nu_C to increase from $Nu_C = 1$ at $EcPr/Da = 0$ to $Nu_C = 3$ at $EcPr/Da \to \infty$. The Nusselt number Nu_H becomes zero at $EcPr/Da$ according to Eq. (62) and passes a discontinuity at $EcPr/Da$ given by Eq. (63). As $EcPr/Da$ increases, Nu_H approaches the horizontal asymptote $Nu_{H\infty} = -3$ from above. The thermal asymmetry is shown to affect the Nusselt numbers stronger at smaller values of $EcPr/Da$.

In this context, it should be noted that Nield et al. [32,33] treated the energy equation, taking into account the axial heat conduction in a slug flow without a heat source, by the method of separation of variables under symmetric heat transfer conditions. With the definitions in this paper, they obtained $Nu = \pi^2/4 = 2.467$ which is independent of the axial position and of the Peclét number. At the thermal symmetry ($\psi_C = \psi_H$), in the fully developed heat transfer region, the present model gives $Nu_C = -Nu_H = 3$, which is independent of the heat source.

5.1.5. Thermal symmetry

For $T_H = T_C = T_W$, the system becomes thermally symmetric, giving

$$\Theta = \frac{T - T_{IN}}{T_W - T_{IN}}, \quad \Psi_H = \Psi_C = \Psi_W = \frac{1}{\Omega}, \tag{64}$$

$$\Psi - \Psi_W = -\left(\frac{y^2}{2} - \frac{2}{\cosh m}\frac{e^{my} + e^{-my}}{2m^2} + \frac{1}{4\cosh^2 m}\left(\frac{e^{2my} + e^{-2my}}{4m^2} + y^2\right)\right) + F(m) \tag{65}$$

with $F(m)$ according to Eq. (31).

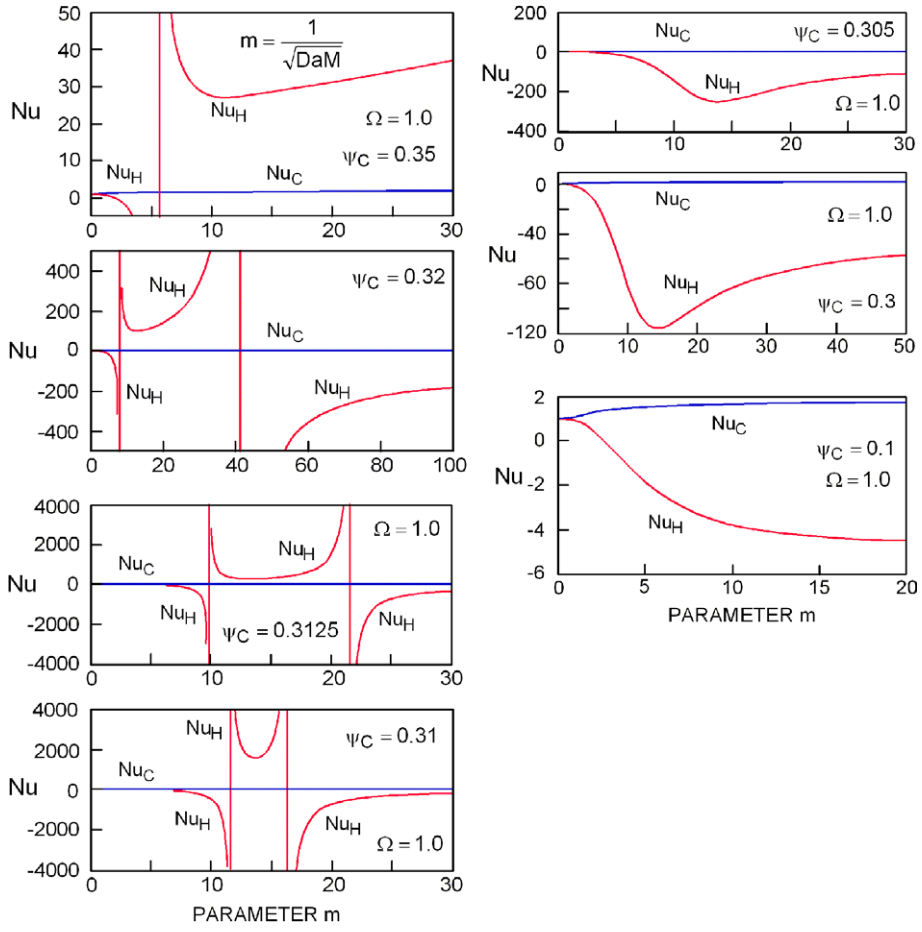

Fig. 9. The Nusselt number Nu_H experiences discontinuity at two values of the parameter m.

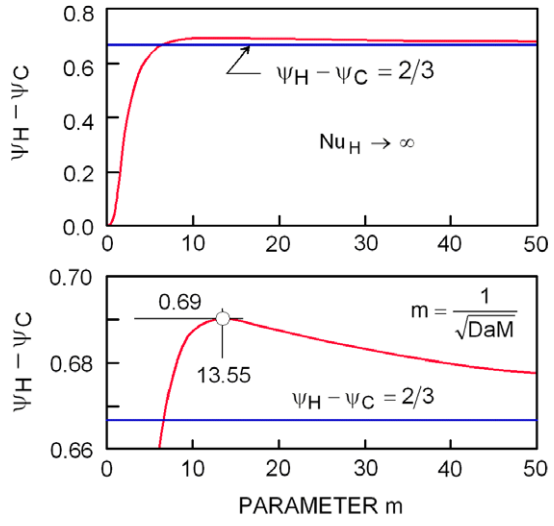

Fig. 10. Dependence of the thermal asymmetry on the parameter m at the discontinuity of Nu_H ($Nu_H \to \infty$).

The corresponding expression for the Fourier heat flux is

$$\frac{qW}{k(T_H - T_{IN})} = -\frac{\partial \Theta}{\partial y} = -\Omega \frac{\partial \Psi}{\partial y}, \tag{66}$$

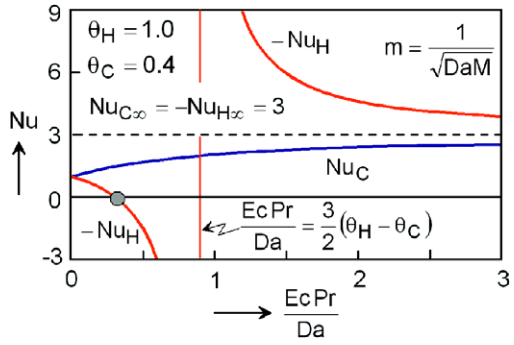

Fig. 11. Nusselt numbers of the plates with fully developed slip flow.

where

$$\left(\frac{\partial \Theta}{\partial y}\right)_{y=+1} = -\frac{EcPrM\Phi^2}{m^2}\left(1 - \frac{3}{2m}\frac{\sinh m}{\cosh m} + \frac{1}{2\cosh^2 m}\right) \tag{67}$$

at the hot plate and

$$\left(\frac{\partial \Theta}{\partial y}\right)_{y=-1} = +\frac{EcPrM\Phi^2}{m^2}\left(1 - \frac{3}{2m}\frac{\sinh m}{\cosh m} + \frac{1}{2\cosh^2 m}\right) \tag{68}$$

at the cold plate, which for large $m = 1/(Da\,M)^{1/2}$ reduce to

$$\left(\frac{\partial\Theta}{\partial y}\right)_{y=+1} = -\frac{Ec\,Pr}{Da}, \tag{69}$$

$$\left(\frac{\partial\Theta}{\partial y}\right)_{y=-1} = +\frac{Ec\,Pr}{Da}. \tag{70}$$

In the case of thermal symmetry, the porous layer always dissipates the heat across its boundaries at the same rate. The expressions for the Nusselt numbers immediately follow from Eqs. (49) and (50) by setting $\psi_H - \psi_C = 0$.

5.2. Thermally developing region

For the integration of Eq. (19), the parameters m, ψ_H and ψ_C, or m, Ω and θ_C are to be specified. For $m = 0$ there is not a porous insert in the channel, whereas for $\Omega = 1$, the fields of ψ and θ are identical. Since the parameter Ω depends on the parameter m, Eq. (17), a variation of Ω actually results in a variation of the product $EcPrM$. A combination and variation of the parameters m, ψ_H and ψ_C would lead to an almost infinite series of fluid flow and heat transfer arrangements. In the following, only some representative results will be discussed depending on the fluid inlet temperature.

5.2.1. Fluid inlet temperature below the plate temperatures

Fig. 12 shows the temperature profiles for the fluid inlet temperature below the cold plate temperature ($T_{IN} < T_C < T_H$) at $\psi_C = 0.5$. For $m = 0$, an empty channel, the fluid is always heated by the hot plate ($y = +1$). On the contrary, the role of the cold plate ($y = -1$) is ambivalent. At a certain distance from the channel inlet, the cold plate becomes adiabatic and the heat flux changes its direction, Fig. 13. Upstream of this position, the fluid is heated, but downstream it is cooled across this plate. The adiabatic position (AP) establishes along the channel where the minimum of the temperature profile reaches the cold

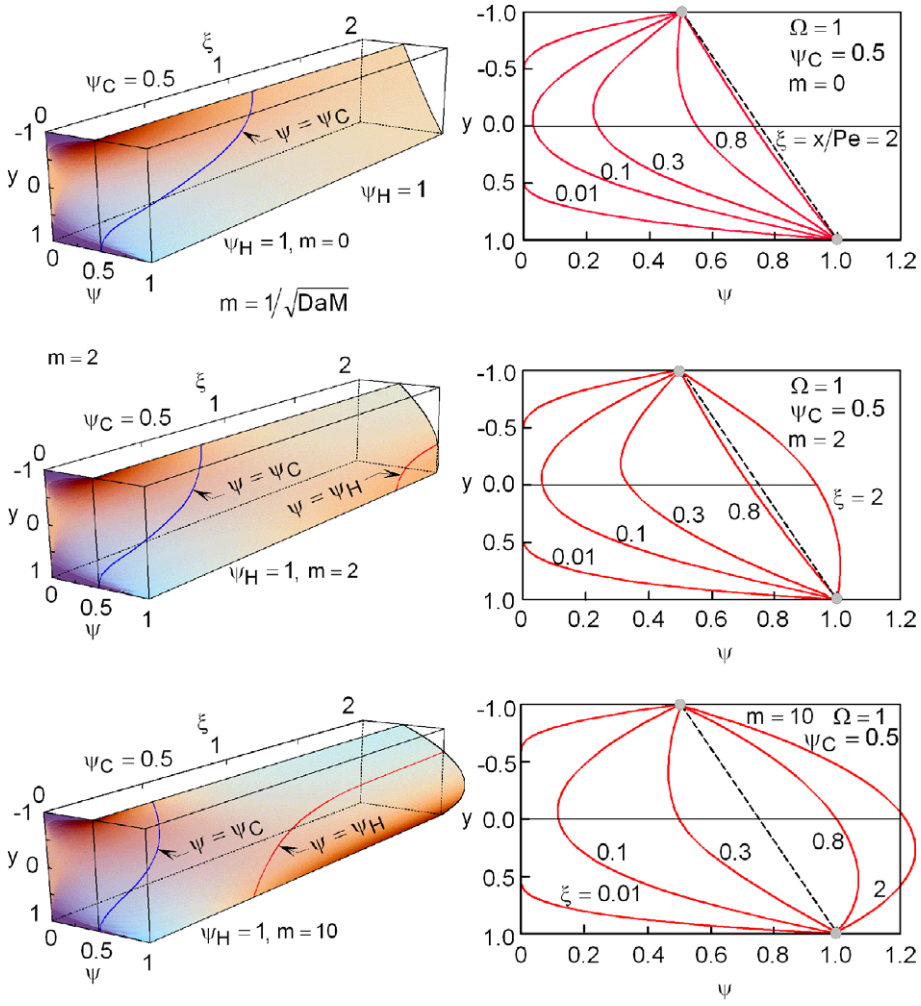

Fig. 12. Temperature profiles in the channel at the fluid inlet temperature below the cold plate temperature $T_{IN} < T_C < T_H$ for $\Omega = 1$, $\psi_C = 0.5$ and selected values of the parameter m.

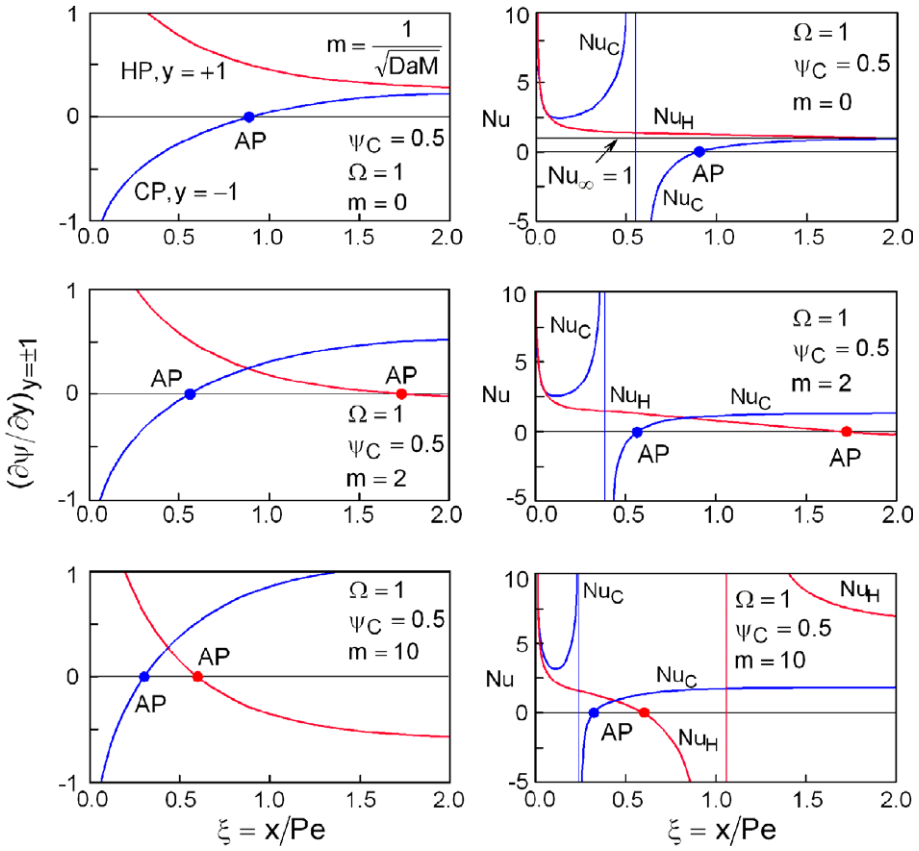

Fig. 13. Heat fluxes and Nusselt numbers on the plates for $T_{IN} < T_C < T_H$.

plate, $(\partial\theta/\partial y)_{y=-1} = 0$. The curve $\psi = \psi_C$ in the 3D-temperature field in Fig. 12 borders the region along the channel where the fluid temperature lies below the cold plate temperature. This curve is obtained by cutting the temperature surface by the plane $\psi = \psi_C$. Downstream of this curve, the fluid dissipates the heat across the cold plate. In the thermally developing region, the temperature is always below the straight line drawn through ψ_C and ψ_H, which represents the fully developed temperature distribution in the empty channel ($m = 0$), Eq. (29), where the heat is transferred from the hot plate to the cold plate through the fluid without affecting its temperature. The Nusselt number Nu_C experiences a discontinuity, becoming zero further downstream and reaches the limit value in the fully developed region, $Nu_{C\infty} = Nu_{H\infty} = 1$. Further details concerning the case of an empty channel are given in an earlier paper [31].

The temperature profiles in the porous layer ($m > 0$) are different from these for $m = 0$. Near the channel inlet, the fluid is heated by both plates as for $m = 0$, but further downstream, the heat flux changes its direction not only on the cold, but also on the hot plate. The corresponding adiabatic positions (AP) move upstream as the parameter m increases. At larger m both Nu_C and Nu_H may become zero and experience discontinuities.

As an example, Fig. 14 illustrates the positions of the adiabatic point and of the vertical asymptote of the Nusselt

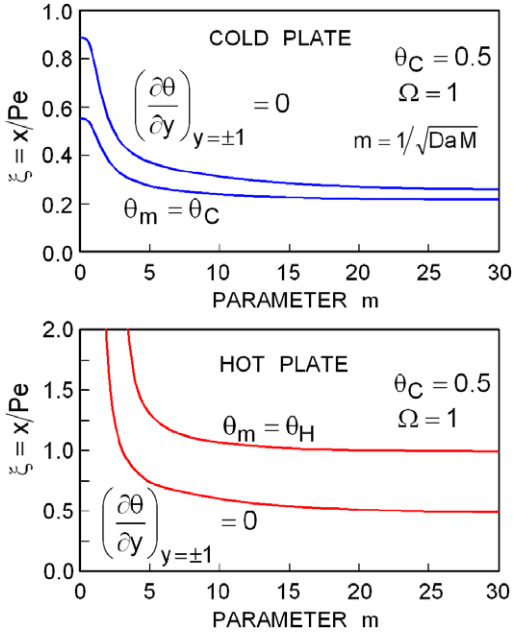

Fig. 14. Position of the adiabatic point and the vertical Nusselt numbers asymptotes for the specified parameter.

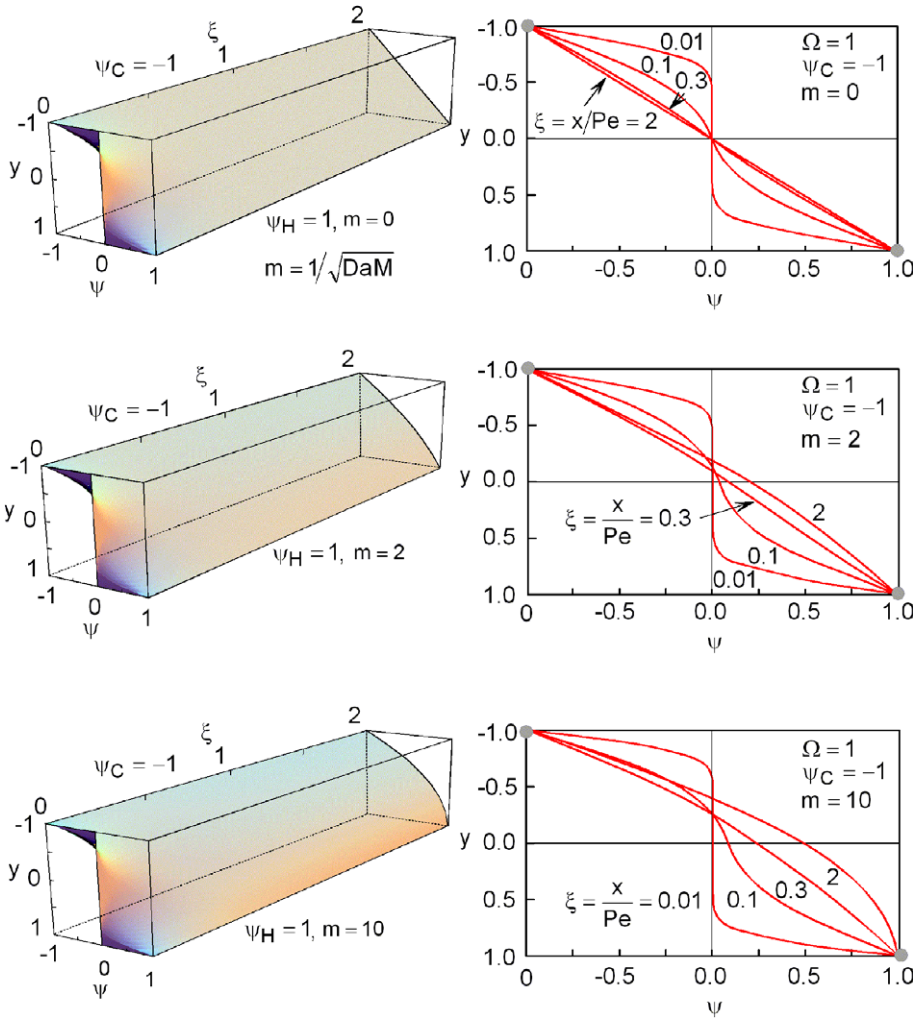

Fig. 15. The same as in Fig. 12, but for the fluid inlet temperature between the plate temperatures, $T_C < T_{IN} < T_H$, at $\Omega = 1$ and $\psi_C = -1$.

numbers for $\Omega = 1$ and $\psi_C = \theta_C = 0.5$ as functions of the parameter m. As the diagrams show, the heat flux always reverses its direction at the cold plate and the Nusselt number Nu_C runs through a discontinuity. The corresponding positions along the channel move upstream as the parameter m increases. At the hot plate, the heat flux reversal and the discontinuity of Nu_H establish only for $m > m_{\min}$. The distance of the adiabatic point from the channel inlet is larger than the distance of the vertical Nusselt asymptote for the cold plate. The situation reverses for the hot plate. In the region of the fully developed heat transfer, the conditions for the adiabatic point are described by Eqs. (37) and (38) and illustrated in Fig. 6.

5.2.2. Fluid inlet temperature between the plate temperatures

Fig. 15 illustrates, as an example, the temperature development at a fluid inlet temperature between the plate temperatures ($T_C < T_{IN} < T_H$) for $\Omega = 1$ and $\psi_C = \theta_C = -1$. In this case, the fluid is always cooled by the cold plate and heated by the hot plate for $m = 0$, and a heat flux reversal does not occur at the plates, Fig. 16. For $m > 0$, the heat flux is larger at the cold plate than at the hot plate. The Nusselt numbers change in the same manner.

5.2.3. Fluid inlet temperature above the plate temperatures

Fig. 17 visualises the situation for the fluid inlet temperature above the hot plate temperature, $T_{IN} > T_H > T_C$, at $\Omega = -1$ and $\psi_C = \theta_C = 2$. In this case, only the hot plate can become adiabatic at an axial position x/Pe that depends on the thermal asymmetry $\psi_H - \psi_C$ and the parameters m and Ω, Fig. 18. As follows from the diagrams, the Nusselt number Nu_H jumps from positive infinite to negative infinite at the axial position where the average fluid temperature becomes equal to the plate temperature, $\theta_H - \theta_m = 0$. The cold plate Nusselt number Nu_C decreases monotonically along the flow direction. The thermal behaviour of the system in this case ($T_{IN} > T_H$) is similar to the one in Fig. 13 for $T_{IN} < T_C$. This time, however, the Nusselt number Nu_H experiences the discontinuity.

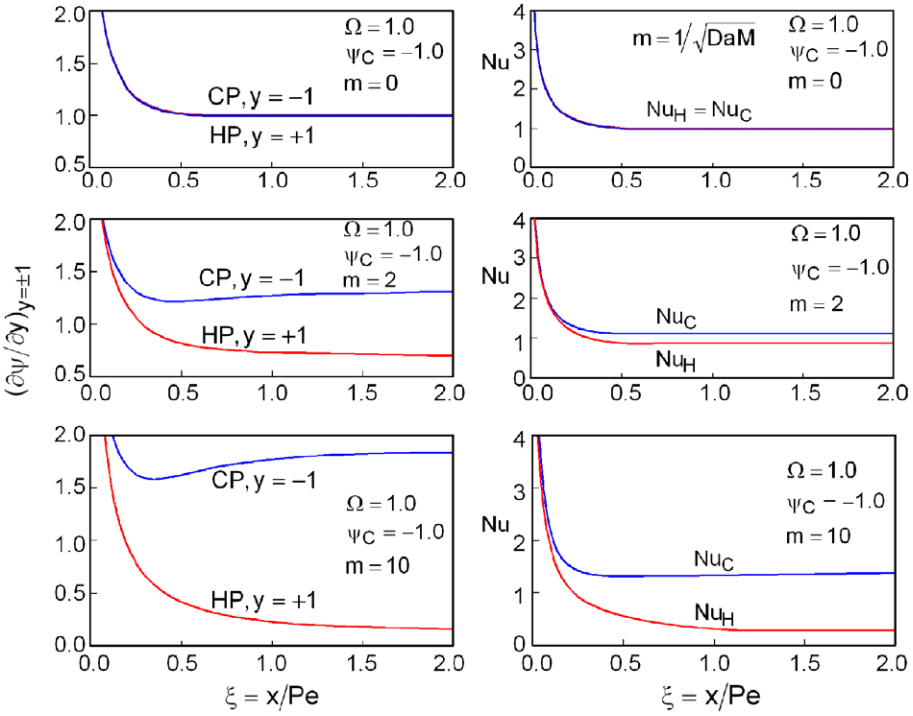

Fig. 16. The same as in Fig. 13, but for $T_C < T_{IN} < T_H$.

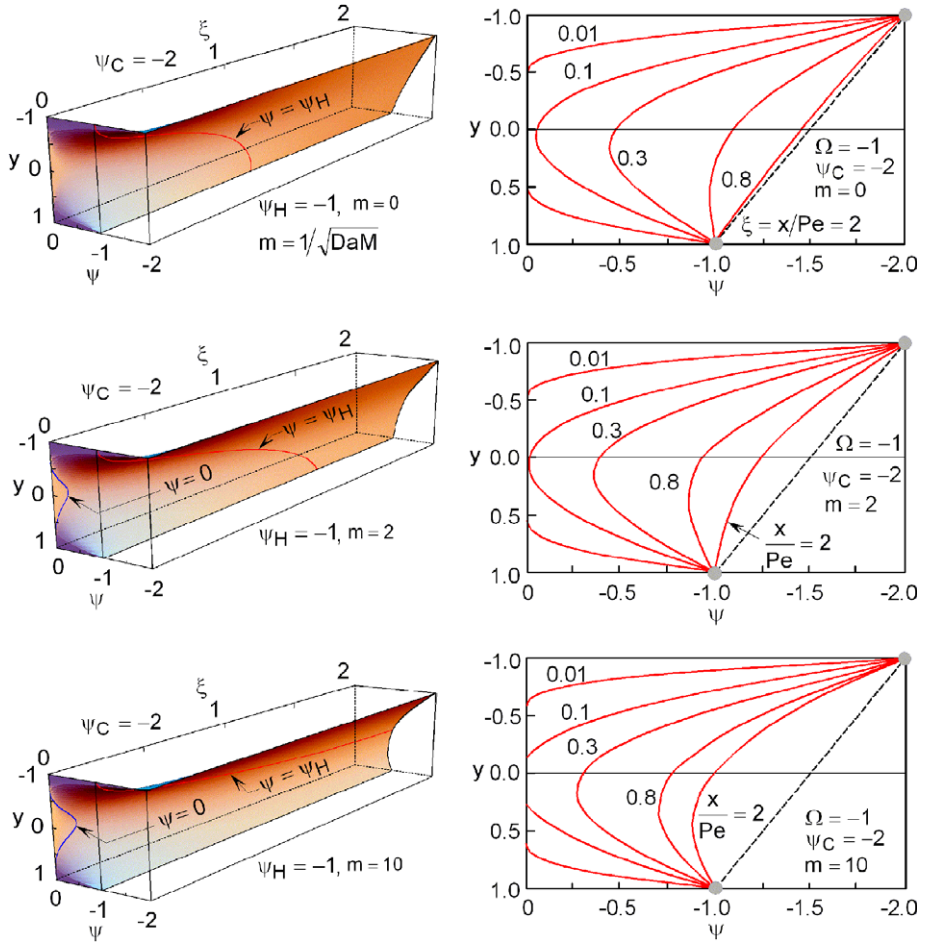

Fig. 17. The same as in Fig. 15, but for the fluid inlet temperature above the hot plate temperature, $T_C < T_H < T_{IN}$, at $\Omega = 1$ and $\psi_C = 2$.

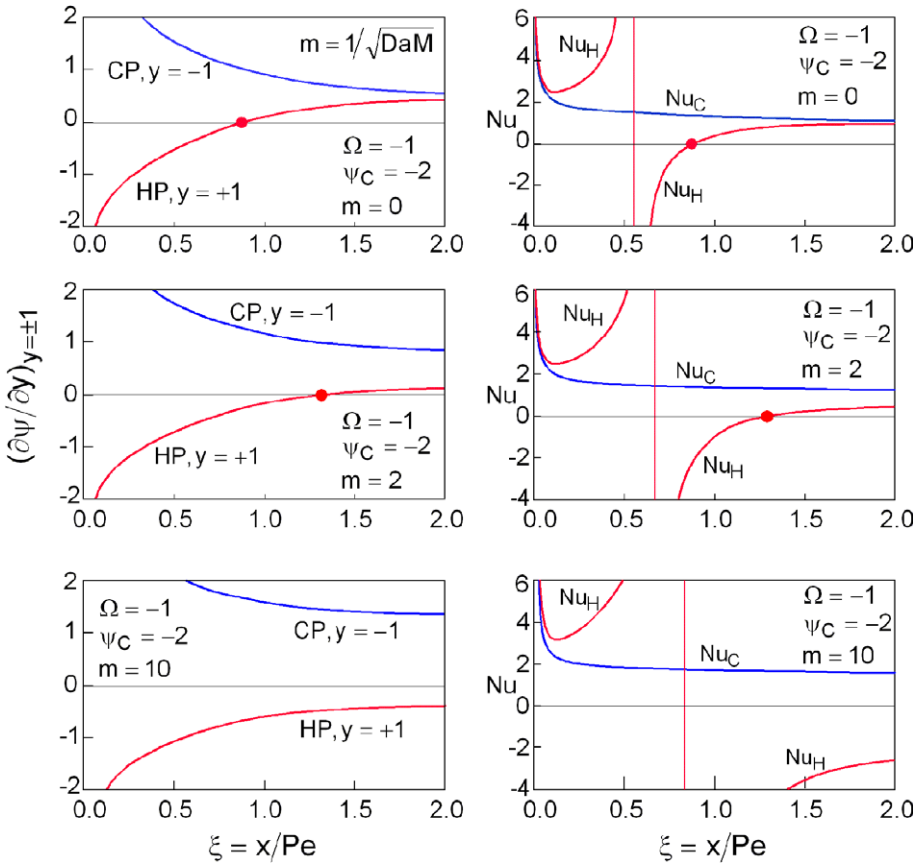

Fig. 18. The same as in Fig. 16, but for $T_C < T_H < T_{IN}$.

6. Conclusions

The temperature distribution in laminar forced convection with Darcy dissipation in a porous channel exposed to a thermal asymmetry results in asymmetric heat fluxes at the channel boundaries. The parameters governing the heat transfer are the non-dimensional quantities like the Darcy, the Eckert and the Peclét number, which is well-known from the literature in the case of symmetric heat transfer. In addition, the thermal asymmetry imposed as the boundary condition substantially affects the heat transfer in the porous medium.

The common figure of heat transfer at thermal symmetry, where, in the developing region, the Nusselt number continually decreases along the flow direction, changes dramatically in the case of a thermal asymmetry. In this case, at least one of the Nusselt numbers may run through a discontinuity and become zero at a certain distance from the channel inlet. This heat transfer behaviour is illustrated in the paper for three characteristic arrangements, namely, for the fluid inlet temperature below, between, and above the temperatures of the plates. In the thermal developed region, analytical equations are obtained for the Nusselt numbers and illustrated for some sets of the process parameters. Like in the developing, also in the thermally developed region, one of the Nusselt numbers may experience a discontinuity thereby jumping from infinite positive to infinite negative, or vice versa, and the corresponding plate kept at constant temperature may simultaneously become adiabatic.

After this paper has been submitted for publication, two publications have appeared in the area of fluid flow and heat transfer in porous media. Minkowycz and Haji-Sheikh [34] deal with the heat transfer in parallel plates and circular porous passages with axial heat conduction and symmetric thermal boundary conditions. The paper by Chandesris and Jamet [35] is devoted to fluid flow in a composed flat channel.

References

[1] A. Bejan, I. Dincer, S. Lorente, A.F. Miguel, A.H. Reis, Porous and Complex Flow Structures in Modern Technologies, Springer, New York, 2004.
[2] M. Kaviany, Principles of Heat Transfer in Porous Media, Springer, New York, 1991.
[3] D.A. Nield, A. Bejan, Convection in Porous Media, second ed., Springer, New York, 1999.
[4] A. Bejan, Convection Heat Transfer, Wiley, New York, 1984.
[5] K. Vafai (Ed.), Handbook of Porous Media, Marcel Dekker, New York, 2000.
[6] V.S. Travkin, I. Catton, Porous media transport description – non-local, linear and non-linear against effective thermal/fluid properties, Advances in Colloid and Interface Science 76–77 (1998) 389–443.

[7] W.G. Gray, C.T. Miller, Thermodynamically constrained averaging theory approach for modelling flow and transport phenomena in porous medium systems: 1. Motivation and overview; C.T. Miller, W.G. Gray: 2. Foundation,Advances in Water Resources 28 (2005), pp. 161–202.
[8] J. Bear, Y. Bachmat, Introduction to Modelling of Transport Phenomena in Porous Media, Kluwer Academic Publishers, Dordrecht, 1990.
[9] S. Whitaker, Coupled transport in multiphase systems: A theory of drying, Advances in Heat Transfer 31 (1998) 1–104.
[10] M. Kaviany, Laminar flow through a porous channel bounded by isothermal parallel plates, Int. J. Heat Mass Transfer 28 (1985) 851–858.
[11] K. Vafai, S.J. Kim, Forced convection in a channel filled with a porous medium: An exact solution, ASME J. Heat Transfer 111 (1989) 1103–1106.
[12] D.A. Nield, S.L.M. Junqueira, J.L. Lage, Forced convection in a fluid-saturated porous-medium channel with isothermal or isoflux boundaries, J. Fluid Mech. 322 (1996) 201–214.
[13] D.A. Nield, A.V. Kuznetsov, M. Xiong, Thermally developing forced convection in a porous medium: Parallel plate channel with walls at uniform temperature, with axial conduction and viscous dissipation effects, Int. J. Heat Mass Transfer 46 (2003) 643–651.
[14] A.A. Mohamad, Heat transfer enhancement in heat exchangers fitted with porous media. Part I: constant wall temperature, Int. J. Thermal Sci. 42 (2003) 385–395.
[15] A. Haji-Sheikh, K. Vafai, Analysis of flow and heat transfer in porous media imbedded inside various shaped ducts, Int. J. Heat Mass Transfer 47 (2004) 1889–1905.
[16] A. Haji-Sheikh, Estimation of average and local heat transfer in parallel plates and circular ducts filled with porous materials, ASME J. Heat Transfer 126 (2004) 400–409.
[17] D.-Y. Lee, K. Vafai, Analytical characterization and conceptual assessment of solid and fluid temperature differentials in porous media, J. Heat Mass Transfer 42 (1999) 423–435.
[18] D.A. Nield, A.V. Kuznetsov, Local thermal nonequilibrium effects in forced convection in a porous medium channel: a conjugate problem, Int. J. Heat Mass Transfer 42 (1999) 3245–3252.
[19] S.J. Kim, S.P. Jang, Effects of the Darcy number, the Prandtl number, and the Reynolds number on local thermal non-equilibrium, Int. J. Heat Mass Transfer 45 (2002) 3885–3896.
[20] M. Prat, Modelling of heat transfer by conduction in a transition region between a porous medium and an external fluid, Transp. Porous Media 5 (1990) 71–95.
[21] D.A. Nield, A note on the modelling of local thermal non – equilibrium in a structured porous medium, Int. J. Heat Mass Transfer 45 (2002) 4367–4368.
[22] W.J. Minkowycz, A. Haji-Sheik, K. Vafai, On departure from local thermal equilibrium in porous media due to a rapidly changing heat source: the Sparrow number, Int. J. Heat Mass Transfer 42 (1999) 3373–3385.
[23] D.A. Nield, A.V. Kuznetsov, M. Xiong, Effect of local thermal non-equilibrium on thermally developed forced convection in a porous medium, Int. J. Heat Mass Transfer 42 (2002) 4949–4955.
[24] J. Mitrovic, B. Maletic, Effect of thermal asymmetry on heat transfer in a laminar annular flow, Chem. Eng. Technol. 28 (2005) 1144–1150.
[25] S. Mahmud, R.A. Fraser, Flow, thermal, and entropy generation characteristics inside a porous channel with viscous dissipation, Int. J. Thermal Sci. 44 (2005) 21–32.
[26] M. Xiong, A.V. Kuznetsov, Forced convection in a Couette flow in a composite duct: An analysis of thermal dispersion and non-Darcian effects, J. Porous Media 3 (2000) 245–255.
[27] J. Mitrovic, B. Maletic, Effect of thermal asymmetry on laminar forced convection heat transfer in a porous annular channel, Chem. Eng. Technol. 29 (2006) 750–760.
[28] S. Wolfram, The Mathematica Book, fourth ed., Cambridge University Press, Cambridge, UK.
[29] J. Lahjomri, A. Oubarra, A. Alemany, Heat transfer by laminar Hartmann flow in thermal entrance region with a step change in wall temperature: the Graetz problem extended, Int. J. Heat Mass Transfer 45 (2002) 1127–1148.
[30] J. Lahjomri, A. Oubarra, Analytical solution of the Graetz problem with axial conduction, ASME J. Heat Transfer 121 (1999) 1078–1083.
[31] J. Mitrovic, B. Maletic, B. Bačlić, Some peculiarities of the asymmetric Graetz problem, Int. J. Eng. Sci. 44 (2006) 436–455.
[32] D.A. Nield, J.L. Lage, The role of longitudinal diffusion in fully developed forced convective slug flow in a channel, Int. J. Heat Mass Transfer 41 (1998) 4375–4377.
[33] D.A. Nield, A.V. Kuznetsov, Effect of heterogeneity in forced convection in a porous medium: parallel plate channel or circular duct, Int. J. Heat Mass Transfer 43 (2000) 4119–4134.
[34] W.Y. Minkowycz, A. Haji-Sheik, Heat transfer in parallel plates and circular porous passages with axial conduction, Int. J. Heat Mass Transfer 49 (2006) 2381–2390.
[35] M. Chandesris, D. Jamet, Boundary conditions at a planar fluid-porous interface for a Poiseuille flow, Int. J. Heat Mass Transfer 49 (2006) 2137–2150.